

PAPER • OPEN ACCESS

## On modelling viscoplastic behavior of the solidifying shell in the funnel-type continuous casting mold

To cite this article: A Vakhrushev *et al* 2019 *IOP Conf. Ser.: Mater. Sci. Eng.* **529** 012081

View the [article online](#) for updates and enhancements.

# On modelling viscoplastic behavior of the solidifying shell in the funnel-type continuous casting mold

A Vakhrushev<sup>1</sup>, A Kharicha<sup>1</sup>, M Wu<sup>2</sup>, A Ludwig<sup>2</sup>, G Nitzl<sup>3</sup>, Y Tang<sup>3</sup>, G Hackl<sup>3</sup>, J Watziger<sup>4</sup>, C M G Rodrigues<sup>2</sup>

<sup>1</sup>Christian-Doppler Lab for Metallurgical Applications of Magnetohydrodynamics, University of Leoben, Franz-Josef-Str. 18, A-8700 Leoben, Austria

<sup>2</sup>Chair of Simulation and Modeling of Metallurgical Processes, University of Leoben, Franz-Josef-Str. 18, A-8700 Leoben, Austria

<sup>3</sup>RHI Magnesita, Austria

<sup>4</sup>Primetals Technologies, Austria

E-mail: alexander.vakhrushev@unileoben.ac.at

**Abstract.** As it is known from literature, the metals tend to follow a viscoplastic law at high temperatures. Thereby, based on the authors' previous developments to simulate the behavior of the equiaxed crystals packed bed, a viscoplastic stress model is applied to the thin slab casting process. The model is reduced to the single phase mixture formulation for faster and robust simulations. In this idea, the solidifying shell represents a 'creeping solid' and the Norton-Hoff type stress model is formulated with the model parameters obtained experimentally. A coupling procedure is established to converge the non-linear terms. The influence of the stress model parameters is investigated. Next the model is applied for the simulation of the thin slab casting to improve a previously developed technique: a viscoplastic rheology is applied to calculate the motion of the solidifying melt instead of imposing the velocities of the mush. The simulation results show that the most deformations happen at the funnel part of the mold, causing highest strain rates and the significant drop of the viscoplastic 'apparent viscosity' according to the Norton-Hoff law. The solid shell velocities are mostly uniform at the straight parts of the strand but a slight acceleration of the shell is observed along the funnel surface. Strong compression / expansion zones are detected at the funnel part, which could lead to defects formation. The solid shell thickness was successfully predicted as well and compared to the previous work by the authors.

## 1. Introduction

Following the pioneering work of Merton C. Flemings [1] it is well known that the properties of the alloys can vary drastically at their semi-solid state, thereby allowing the deformations to form and accumulate under mechanical strains during the casting process. The aim of the current work is to make an attempt to track the mechanical behavior of the solidifying shell during continuous casting in a funnel-type thin slab mold by employing a viscoplastic stress model.

Very recently the co-authors simulated the twin-roll casting process using viscoplastic approach [2, 3] within frames of the two-phase Eulerian–Eulerian volume-averaging model [4]. An inoculated Al–4wt%Cu alloy (typically showing globular solidification) was studied in regard of the partially solidified shell compression and the corresponding effects on the macrosegregation distribution.



Compression-induced expulsion of the melt against casting direction was observed, which led to remelting of the mixture and strong contribution to the centerline macrosegregation. A 2D simplification was done due to large width / thickness ratio of the twin-roll strip, which allowed keeping the mesh size below  $10^4$  cells.

In current work the viscoplastic Norton-Hoff type stress is applied to model a complex process of the thin slab continuous casting and the first results are discussed. The advantage of the proposed approach is using finite-volume formulation for both solid shell mechanical behavior and for the strong melt flow. The latter is typically excluded in most studies on the mechanical stress calculations by simplifying to a plug-type. In the presented study the flow phenomenon is fully considered. To make the numerical procedure stable, computationally effective and robust the following simplifications are done: (i) constant parameters of the viscoplastic model are assumed; (ii) mixture formulation is employed resulting in a single phase formulation.

The presented work considers a full 3D model of a submerged entry nozzle (SEN), a funnel-type thin slab mold (880 mm in height) and strand part (3000 mm along casting direction). The boundary layers are introduced to correctly predict near-wall flow and heat flux. Thus the typical numerical grid in the present work can reach up to 10 million finite volume (FV) elements. Additionally a strong flow in the SEN region drastically limited the efficiency of the time marching algorithm. Taking this into account, the multiphase approach was found inappropriate for transient full-scale industrial simulation.

The mixture volume averaging, based on the previous report in Vakhrushev et al. [5], was extended by combining a liquid viscous stress with a viscoplastic one for the solid phase. Next the details of the numerical model and algorithm as well as the simulation results are presented and discussed.

## 2. Numerical model

### 2.1. Viscoplastic model for the solidified shell

As it was previously described, a numerical Eulerian-Eulerian model was suggested to simulate the behavior of the packed bed of equiaxed crystals [2, 3]. The metals at the temperatures higher than  $2/3$  of their melting absolute (according to the book of Rappaz, Bellet and Deville, p. 309 [6]) are known to follow a viscoplastic law. Thereby based on the authors' developments and experience the viscoplastic stress model was applied to the thin slab casting process. However, to make it more robust it was simplified to a single phase 'mixture' approach. The compressibility of the solid skeleton suggested by Fachinotti et al. [7] and used in Bellet [8] was excluded at this stage from the model as well. Thus the solidifying shell was represented as a 'creeping solid' in incompressible formulation. The Norton-Hoff viscoplastic stress model [6] is formulated as follows:

$$\boldsymbol{\sigma}^{vp} = 2K(\sqrt{3} \dot{\epsilon}_{eq})^{m-1} \text{dev}(\dot{\boldsymbol{\epsilon}}), \quad (1)$$

where the viscoplastic consistency  $K$  and strain rate sensitivity  $m$  are the model parameters obtained experimentally;  $\dot{\boldsymbol{\epsilon}}$  is the strain rate tensor (the symmetric part of the velocity gradient). The equivalent strain rate is defined from the deviatoric part of  $\dot{\boldsymbol{\epsilon}}$  and reflects the dynamic load rate at the local point:

$$\dot{\epsilon}_{eq} = \sqrt{\frac{2}{3} \text{dev}(\dot{\boldsymbol{\epsilon}}) : \text{dev}(\dot{\boldsymbol{\epsilon}})}. \quad (2)$$

For a more convenient formulation the 'effective' or 'apparent' viscoplastic viscosity is introduced:

$$\mu^{vp} = K(\sqrt{3} \dot{\epsilon}_{eq})^{m-1}. \quad (3)$$

The main difference between the liquid and the viscoplastic viscosity is that the latter depends on the current flow situation (also called rate of load), expressed in the current model by the equivalent strain rate. Moreover since the strains and stresses are integrated into the 'apparent' viscosity calculation, the coupling procedure is required to converge the non-linear terms. This involves the following steps: (i) estimate the strain rate; (ii) update the equivalent strain and the viscoplastic viscosity; (iii) come to a

new solution of the flow / heat transfer equation system based on the latest estimation of the stress distribution; (iv) repeat procedure applying under-relaxation on pressure and velocity fields as well as on the effective viscosity. An additional step is to limit the maximum viscoplastic viscosity value due to stability issues. Enhanced treatment of the stresses model will be applied in the future to remove any restrictions.

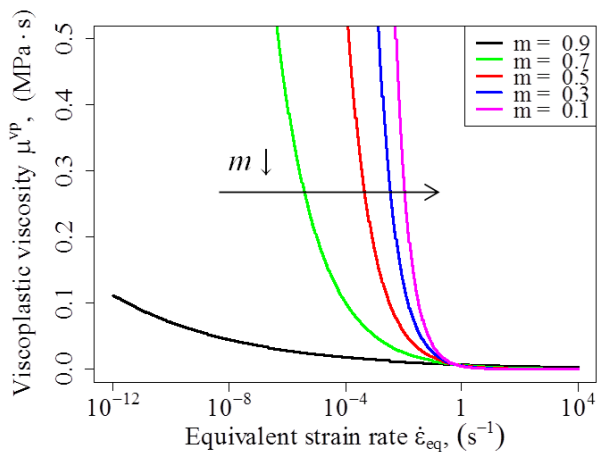


**Figure 1.** Viscoplastic viscosity  $\mu^{VP}$  vs. equivalent strain rate  $\dot{\epsilon}_{eq}$  as in (3) for different strain rate sensitivities  $m$ ; consistency  $K=65.16$  (Table 1).

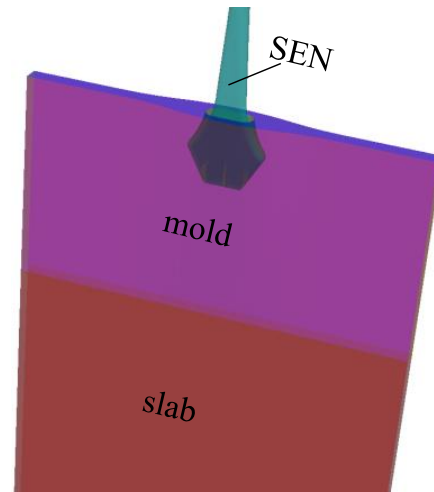


**Figure 2.** Simulation domain: the boundary conditions are given in Vakhrushev et. al [5]. Inlet / casting parameters are in Table 1.

The basic parameters of the viscoplastic deformation model were selected according to the model from Kozłowski et. al [10] (see Table 1). As it is indicated in Figure 1, for equivalent strain rates below  $1 \text{ s}^{-1}$ , the viscoplastic viscosity increases dramatically as the parameter  $m$  decreases.

## 2.2. General equations of motion

In the incompressible mixture volume average approach the momentum equation is formulated as

$$\rho \left[ \frac{\partial \vec{u}}{\partial t} + \nabla \cdot (\vec{u} \otimes \vec{u}) \right] = \nabla \cdot [\text{dev}(\boldsymbol{\sigma}_{\text{tot}}) - p\mathbf{I}], \quad (4)$$

where the total stress  $\boldsymbol{\sigma}_{\text{tot}}$  is decomposed into deviatoric and hydrostatic parts; the pressure equilibrium ( $p_\ell = p_s = p$ ) is assumed between the phases. The deviatoric part of the total stress tensor is calculated by combining the viscoplastic formulation (1) and one for the Newtonian liquid, yielding:

$$\text{dev}(\boldsymbol{\sigma}_{\text{tot}}) = f_s \cdot \boldsymbol{\sigma}^{VP} + f_\ell \cdot 2\mu_\ell \cdot \text{dev}(\boldsymbol{\epsilon}). \quad (5)$$

It is worth mentioning that for the sake of simplification, turbulence modelling using RANS, LES and further approaches was excluded in this work. Instead the ‘coarse DNS’ approach was utilized on a fine numerical grid ( $\sim 10$  million cells) by assuming the liquid viscosity  $\mu_\ell$  to be constant.

## 2.3. Latent heat advection

The latent heat advection is crucial for the solid shell formation [5, 9]; its formulation is re-derived here since the mixture approach gives no solid phase velocities distribution. For the total enthalpy  $H$

$$H = \int C_p \cdot dT + f_\ell \cdot L \quad (6)$$

the energy equation is taken in its general advection-diffusion form

$$\rho \left[ \frac{\partial H}{\partial t} + \nabla \cdot (\vec{u}H) \right] = \nabla \cdot \lambda \nabla T. \quad (7)$$

By utilizing (6) the latent heat advection term can be derived from (7) in a following form:

$$S_e = \rho L \left[ \frac{\partial f_s}{\partial t} + \nabla \cdot (f_s \cdot \vec{u}) \right]. \quad (8)$$

The comparison is done with the results obtained using the previous formulation [5, 9]:

$$S_e = \rho L \left[ \frac{\partial f_s}{\partial t} + \nabla \cdot (f_s \cdot \vec{u}_s) \right] \quad (9)$$

The difference between (8) and (9) is in using averaged velocity  $\vec{u}$  instead of the solid ones  $\vec{u}_s$ .

### 3. Simulation results

Next the model was applied for the simulation of the thin slab caster to enhance a previously developed model [5]. Instead of the imposed solid shell velocities a viscoplastic rheology of the mush was applied to calculate the motion of the solidifying melt. The material parameters of the alloy 0.06C 0.1Ni 0.13Mn 0.1Si 0.08Cu 0.035Al 0.015P 0.012S are summarized in Table 1: the strain rate sensitivity coefficient  $m$  is taken from Ludwig et al [3] and corresponds to the temperature mid-range of the experimental measurements for the Model IA in Kozłowski et. al [10]. The same model is selected to estimate the viscoplastic consistency  $K$ . Since a strong non-linear term can ‘destroy’ the convergence of the solution, the viscoplastic kinematic viscosity  $\eta^{vp} = \mu^{vp}/\rho$  was limited to  $10^{10}$  m<sup>2</sup>/s allowing the numerical procedure to converge without any special technique. Additionally, the increased casting speed of 5.5 m/min was used in this study.

**Table 1.** Material properties used in the study. For the domain geometry and casting conditions details please refer to Vakhrushev et al. [5].

Properties	Symbols	Units	Quantities
Density	$\rho = \rho_\ell = \rho_s$	kg · m <sup>-3</sup>	6998.49
Specific heat	$C_p = C_p^\ell = C_p^s$	J · kg <sup>-1</sup> · K <sup>-1</sup>	838.2
Thermal conductivity	$\lambda = \lambda_\ell = \lambda_s$	W · m <sup>-1</sup> · K <sup>-1</sup>	35
Liquid dynamic viscosity	$\mu_\ell$	Pa · s	0.0054
Latent heat of fusion	$L$	J · kg <sup>-1</sup>	243000
Viscoplastic consistency	$K$	Pa · s <sup><math>m</math></sup>	65.16
Strain rate sensitivity	$m$	–	0.138
Casting velocity	$\vec{u}_{pull}$	m/min	5.5
Casting (inlet) temperature	$T_{cast}$	K (°C)	1825 (1552)
Liquidus temperature	$T_{liquidus}$	K (°C)	1798 (1525)
Solidus temperature	$T_{solidus}$	K (°C)	1755 (1482)

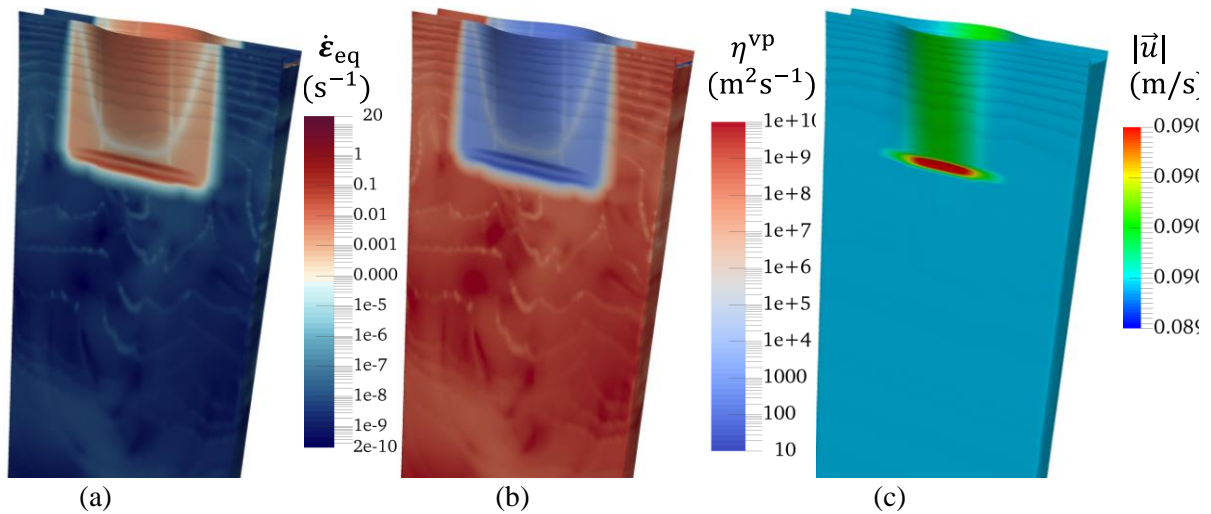


**Figure 3.** The simulation results of the thin slab casting using viscoplastic deformation model: (a) equivalent strain rate; (b) kinematic viscoplastic viscosity  $\eta^{vp}$ ; (c) solid shell velocities.

The results of the thin slab simulation are shown in Figure 3: the distribution of the model parameters is displayed at the iso-surface of 90% solid fraction. The solid shell iso-surface is scaled up in thickness direction by a factor of 4 for better results representation. It was found that the most deformation happens at the funnel part of the mold, causing highest strain rate as it is observed in Figure 3-a. Viscoplastic viscosity drops at the region of the highest strain according to the Norton-Hoff law. Solid shell velocities are uniform at the straight parts of the mold and strand (see Figure 3-c); slight acceleration of the shell is observed along the funnel surface. Solid shell thickness was successfully predicted as well and is analyzed next in Figure 4.

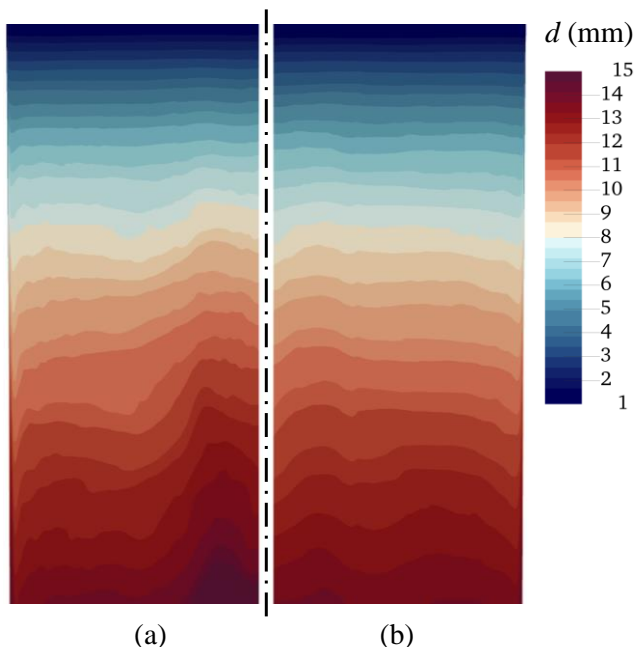


**Figure 4.** Comparison of the solid shell thickness  $d$  distribution along the wide face: (a) corresponds to the previous model [5]; (b) shows the results for the new viscoplastic stress model been applied.

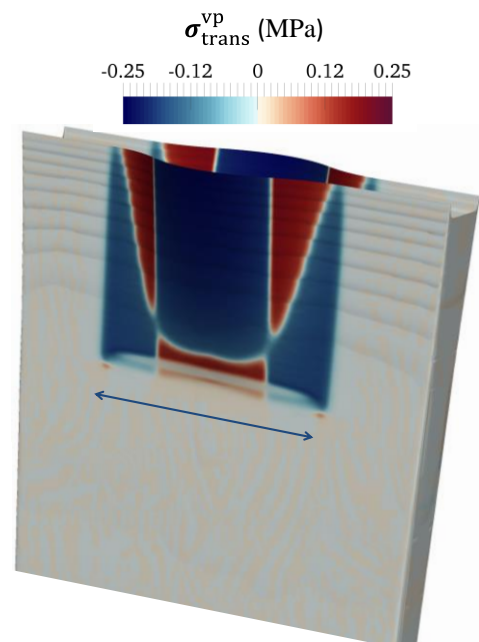


**Figure 5.** Distribution of the transversal component of the viscoplastic stress tensor  $\sigma^{vp}$ : compression is in red colors and expansion is in blue.

In Figure 4 the solid shell thickness is compared for both models. The comparison is shown at the wide face of the slab. It is observed that along the casting (vertical) direction the shell thickness is generally lower when the viscoplastic model is applied, but only a slight difference occurs. However a more distinct pattern between both cases is detected in the transversal distribution: in the case of the pre-estimated solid velocities [5] the shell is thicker in the central part of the wide face, whereas in the new approach it is slightly thicker in the lower part of the domain at the 1/4 of the width from the narrow side. It should be noted that at the mold region of the domain no differences between the two models could be detected. The deviation can be described by recalling the previously derived formulation (9) of the latent heat release term [5, 9], where the advection term is based on the prescribed solid velocities  $\vec{u}_s$  and the new one, which according to (8) depends on the mixture velocity. Despite the model differences the shell thickness deviation is not dramatic.

The transversal component of the stress tensor acting along the wide direction of the shell surface (90% solid) is investigated as shown in Figure 5. Strong compression / tension areas are detected especially along the curved funnel part of the mold cavity. It was found that the shell is under tension horizontally at the central and outer parts of the funnel (check for  $\sigma_{\text{trans}}^{\text{vp}} < 0$  in Figure 5).

The critical tensile values in the simulation lie in the range of 250 kPa. The ultimate tensile stress (UTS) for the steel alloys is typically 500-1000 MPa at room temperature conditions. However the UTS is strongly temperature and alloy dependent. As reported by Outinen and Mäkeläinen[11] and recently reviewed by Wang and Lui[12], the strength properties of the steel drop to 5-10% level at the temperature 1000°C. Extrapolating experimental data[11, 12] up-to 1500°C we obtain the lower range for the UTS of 0,5-1 MPa which makes a simulation value (250 kPa) close to the critical one. Thereby at the upper part of the mold the hot jet impingement and local remelting can lead to the weakening of the solidifying shell strength and end-up with its rupture.

However, as mentioned previously, in the developed model the viscoplastic viscosity  $\mu^{\text{vp}}$  is limited for the simulation stability purposes, thus the maximum tensile stress values currently cannot be judged realistically. Thereby it is a key point for the next studies.

#### 4. Conclusions

In the presented study a viscoplastic stress model was newly introduced to model the thin slab casting process based on the volume-averaged mixture approach. The Norton-Hoff type stress tensor was incorporated for the two-phase region. The influence of the strain rate sensitivity parameter on the viscoplastic effective viscosity was studied.

Full 3D simulation was performed for the numerical domain including the submerged entry nozzle, the funnel-type thin slab mold and 3 m strand part along casting direction below the molds exit. The liquid flow was combined with the heat transfer and solidification based on the viscoplastic stress calculations. The modelling results were verified with previous simulations obtained using static solid velocities distribution; the comparison showed slight deviations due to different latent heat advection term formulations. However the advantage of the newly suggested approach is that it ‘naturally’ tracks the evolution of the solid shell motion based on the local load rate status.

The algorithm’s stability was investigated and an enhanced numerical treatment of the strongly non-linear terms (reported in the literature) has to be applied in the future to realistically estimate the tensile stress values and to compare it against the temperature dependent ultimate tensile stress.

The developed numerical model can be directly applied for industrial process simulations.

#### 5. Acknowledgments

The financial support by the Austrian Federal Ministry of Economy, Family and Youth and the National Foundation for Research, Technology and Development is gratefully acknowledged.

#### References

- [1] Flemings M C 1991 *Metall. Trans. A* **22A** 957
- [2] Ludwig A, Vakhrushev A, Holzmann T, Wu M and Kharicha A 2015 *IOP Conf. Ser.: Mater. Sci.*

*Eng.* **84** 012102

- [3] Ludwig A, Vakhrushev A, Wu M, Holzmann T and Kharicha A 2015 *Trans. Indian Inst. Met.* **68** 1087
- [4] Rodrigues C M G, Ludwig A, Kharicha A and Wu M. 2018 *Trans. Indian Inst. Met.* **71** 2645
- [5] Vakhrushev A, Wu M, Ludwig A, Tang Y, Hackl G and Nitzl G 2014 *Metall. Mater. Trans. B* **45B** 1024
- [6] Rappaz M, Bellet M and Deville M. *Numerical modeling in materials science and engineering*. 2003 New York: Springer
- [7] Fachinotti V D, Le Corre S, Triolet N, Bobadilla M and Bellet M 2006 *Int. J. Numer. Methods Eng.* **67** 1341
- [8] Bellet M 2007 AIP Conf. Proc. **908:1** 1369
- [9] Wu M, Vakhrushev A, Ludwig A and Kharicha A 2016 *IOP Conf. Ser.: Mater. Sci. Eng.* **117** 012045
- [10] Kozłowski P F, Thomas B G, Azzi J A, Wnag H 1992 *Metall. Mater. Trans B* **23A** 903
- [11] Outinen J, Mäkeläinen P 2004 *Fire Mater.*, **28** 237
- [12] Wang F, Lui E M 2016 *J. Steel Struct. Constr.* **2:2** 1000123